Hittite Journal of Science and Engineering, 2023, 10 (1) 83-90
ISSN NUMBER: 2148-4171
DOI: 10.17350/HJSE19030000295

FliA-Dependent Surface Macromolecules Promote Initial Biofilm Development of *Escherichia coli* by Influencing the Bacterial Surface Properties

Fatma Pinar Gordesli Duatepe
Izmir University of Economics, Department of Genetics and Bioengineering, Izmir, Turkey

Article History:
Received: 2023/02/13
Accepted: 2023/03/13
Online: 2023/03/31

***Correspondence to**: Fatma Pinar Gordesli Duatepe, Izmir University of Economics, Department of Genetics and Bioengineering, 35330, Izmir, Turkey.*
E-Mail: pinar.gordesli@iue.edu.tr
Phone: +90 (232) 488 9824

ABSTRACT

FliA is an important regulatory component for the synthesis of surface macromolecules which are involved in motility and biofilm development of *Escherichia coli*. In this study, the roles of FliA-dependent surface macromolecules in *E. coli* surface tension, surface heterogeneity and surface roughness, and initial biofilm development consisting of reversible and irreversible adhesion were investigated using *E. coli* MG1655 wild-type strain and *fliA* gene deleted mutant strain. Negative Gibbs free energy change values calculated using bacterial surface tensions obtained by a spectrophotometric method showed that both wild-type and mutant cells in water can reversibly adhere to the surface of the model solid, silicon nitride (Si_3N_4). The calculations further showed that bacterial reversible auto-adhesion and co-adhesion were also thermodynamically favorable. In comparison, the reversible adhesion and auto-adhesion capacities of wild-type cells were higher than the mutant cells. Direct measurements by atomic force microscopy (AFM) and thorough analysis of the recorded adhesion data showed that the irreversible adhesion strength of wild-type cells to Si_3N_4 in water was at least 2.0-fold greater than that of the mutants due to significantly higher surface heterogeneity resulting in higher surface roughness for the wild-type cells compared to those obtained for the mutants. These results suggest that strategies aimed at preventing *E. coli* biofilm development should also consider a combined method, such as modifying the surface of interest with a bacterial repellent layer and targeting the FliA and FliA-dependent surface macromolecules to reduce both reversible and irreversible bacterial adhesion and hence the initial biofilm development of *E. coli*.

Keywords:
FliA; *E. coli* biofilm; Gibbs free energy change; Surface heterogeneity; Surface roughness; Adhesion energy; Atomic force microscopy

INTRODUCTION

A variety of aquatic bacteria, including *Escherichia coli*, can attach to both biological and abiotic surfaces and initiate the formation of biofilms, which are surface-bound communities of bacterial cells coated with protective extracellular polymeric substances [1-3]. Biofilms represent a source of water contamination in drinking water supplies [4], and can cause damage to equipment and materials in industrial water systems [5]. In addition, biofilms create specialized environments that confer bacterial tolerance and resistance to antimicrobial agents and enhance intra- and inter-species exchange of antimicrobial resistance (AMR) genes [6] and cause many chronic infections [7]. Biofilms are therefore also a source of antimicrobial resistance, the spread of which among bacteria is currently a global public health challenge [8]. For these reasons, researchers have been investigating biofilms from different perspectives to propose effective methods to eliminate biofilm development on surfaces.

Since many aquatic bacteria can form biofilms and cause infections, it is important to choose a well-known bacterial species that can form biofilms on different surfaces to study the bacterial biofilm development. In this context, *E. coli*, a well-characterized human pathogen that causes intestinal and medical device-related infections [9], is known for its competence to grow into biofilms on biological surfaces and abiotic surfaces such as glass and different metal and plastic surfaces [7-9]. Thus, studies have often used *E. coli* as a paradigm for the investigation of the process of bacterial biofilm development, which usually occurs in a stepwise manner [10-13]. The steps include reversible initial bacterial ad-

hesion to a surface driven mainly by attractive and repulsive physicochemical interactions [14, 15], irreversible initial bacterial adhesion to the surface via binding of surface-associated biomacromolecules to the surface [10-14], biofilm maturation via the increase of biofilm biomass on the surface and secretion of extracellular polymeric substances, and ultimately biofilm dispersion via the detachment of bacteria from the biofilm [10-12]. As can be seen from this process, the starting point of biofilm development is the first contact of the bacterial cell with the surface. For the case of *E. coli*, surface-associated locomotive appendages called flagella propel the cells towards a surface and help them cope with repulsive interactions in the vicinity of that surface [12, 13]. Cells that overcome the repellent barrier and come into contact with the surface use flagella and other surface macromolecules to irreversibly adhere to the surface of interest and to the cells that have already managed to adhere to the surface, thus initiating the biofilm development [12]. However, flagella are not always a key component for the bacterial cell to approach the surface, attach and grow into a biofilm. This is because nonmotile *E. coli* can be transported to a surface with the fluid flow or by the gravitational force leading to the slow deposition of cells onto the surface [3, 11, 12]. Hence cells lacking flagella can still form biofilms via the extracellular macromolecules other than flagella such as curli fimbriae, pili, and other adhesion factors [12]. Curli fimbriae are functional fibers of protein aggregates that promote auto-aggregation and biofilm formation, and pili are hair-like proteinaceous adhesins that have been considered to enable the initial biofilm formation of *E. coli* [10, 11].

In *E. coli*, the master regulator FlhDC activates the transcription of a number of flagellar genes including *fliA* that encodes the alternative Sigma factor FliA [16-18]. FliA transcribes the genes whose expression is required late in flagellar assembly [18]. FliA is not only involved in flagella synthesis, but is also an important regulatory component linking flagella and type 1 pili synthesis [16]. As it was reported that, in *E. coli* LF82 deletion mutant lacking FliA, type 1 pili synthesis, adhesion and invasion decreased dramatically [16]. Although the motility and curli-mediated adhesion have been reported to be inversely coordinated in *E. coli* [18], Congo red depletion was observed to be significantly enhanced by the overexpression of FliA in planktonic *E. coli* cells, indicating increased curli concentration [12]. These findings support the important role of FliA in the synthesis of *E. coli* surface macromolecules that mediate this microbe's motility and adhesion to surfaces.

Although the role of FliA in the regulatory networks of flagella synthesis and motility [16-18], in the regulation of type 1 pili synthesis [16], as well as in the biofilm composition [12] and biofilm architecture [19] of *E. coli* has been unveiled, the role of FliA in the surface properties and initial biofilm development steps of *E. coli* cells has not been systematically investigated, and therefore require further examination. To investigate the role of FliA-dependent surface macromolecules in bacterial surface tension and the reversible initial adhesion capacity of *E. coli*, first the surface tensions of *E. coli* MG1655 wild-type (WT) and FliA mutant cells were determined using a spectrophotometric method. The surface tensions of the bacterial cells were used in the calculations of the Gibbs free energy changes for the reversible bacterial adhesion to the model solid surface, providing the necessary information about whether the reversible bacterial attachment is thermodynamically favorable. Furthermore, the Gibbs free energy changes for bacterial auto-adhesion and co-adhesion were also calculated. To investigate the role of FliA-dependent surface macromolecules in the initial irreversible adhesion of *E. coli*, the most important step taking place at the nano-scale that initiates the biofilm development, as well as the heterogeneity of the surface macromolecules and the roughness of the cell surface, atomic force microscopy (AFM) measurements were performed on the WT cells and FliA mutants.

MATERIAL AND METHODS

Bacterial Strains and Cultures

E. coli K-12 MG1655 WT strain and mutant strain deleted of *fliA* gene (*E. coli* MG1655 Δ*fliA*) were kindly provided by Prof. Dr. Thomas K. Wood, Professor of Chemical Engineering at the Pennsylvania State University. Prior to spectrophotometric and AFM measurements, WT cells and mutants were grown at 37 °C and 170 rpm until the late exponential growth phase in Luria-Bertani broth (LB) and LB supplemented with 50 μg/mL of kanamycin [19], respectively. The cells were then centrifuged 3 times at 3000 rpm for 10 minutes and collected for use in the following experiments.

Determination of Bacterial Surface Tension by Spectrophotometric Measurements

When bacterial cells are maximally dispersed in a liquid, their surface tension should be close to the surface tension of the liquid they are in [20-22]. To apply the aforementioned principle, the protocol developed for the quantitative determination of bacterial surface energies [21, 22] was adapted. Briefly, using predetermined mixing ratios, 0.5 ml of ethanol-water mixtures with known surface tensions (22 to 73 mJ/m²) were prepared at room temperature. Then, 10 μl each of WT and FliA mutant cell suspensions were added to the mixtures and vortexed. After 20 min, the ethanol-water mixtures containing bacteria were centrifuged at 100g for 6 min and 200 μl of the supernatant of each mixtures was added into the wells of the microplates [22]. The

optical density (OD) for each supernatant in the wells of the microplates was then measured (λ = 570 nm) and plotted against the surface tensions of the ethanol-water mixtures. The peak OD values in the plots were obtained by polynomial fitting and the liquid surface tensions corresponding to the peak OD values were evaluated as the surface tensions of the bacterial cells.

Calculation of the Change in the Gibbs Free Energy for Reversible Bacterial Adhesion

The Gibbs free energy change represents the thermodynamic state of a system in terms of its availability or potential to do useful (non-expansion) work in a reversible process. Since the interfacial tension is the free energy per unit surface area required to form an interface between two phases, the interfacial tensions for bacterium-solid (γ_{bs}), bacterium-liquid (γ_{bl}) and solid-liquid (γ_{sl}) interfaces allow for the calculation of the Gibbs free energy change upon the reversible bacterial adhesion to a solid surface in a liquid medium [23-26] as follows:

$$\Delta G_{adhesion} = \gamma_{bs} - \gamma_{bl} - \gamma_{sl} \quad (1)$$

The interfacial tensions given in equation 1 were quantified using the surface tensions of the bacterium (γ_b), solid (γ_s), and the liquid (γ_l) based on the Neumann's equation of state [27] as:

$$\gamma_{bs} = \gamma_b + \gamma_s - 2\sqrt{\gamma_b \gamma_s}\, e^{-\beta(\gamma_b - \gamma_s)^2} \quad (2)$$

$$\gamma_{bl} = \gamma_b + \gamma_l - 2\sqrt{\gamma_b \gamma_l}\, e^{-\beta(\gamma_b - \gamma_l)^2} \quad (3)$$

$$\gamma_{sl} = \gamma_s + \gamma_l - 2\sqrt{\gamma_s \gamma_l}\, e^{-\beta(\gamma_s - \gamma_l)^2} \quad (4)$$

where β is the universal constant (0.0001247 $(mJ/m^2)^{-2}$) [27]. In this study, the model solid was chosen as silicon nitride (Si_3N_4) because the surface potential of Si_3N_4 is similar to the surface potentials of soil and glass [28], which are the substrates to which bacterial cells usually adhere in nature [29]. In addition to its resemblance to a surface to which bacteria adhere in nature, the current and potential use of Si_3N_4 as a biomedical material for different medical applications [30] make it a model inert surface for the studies investigating bacterial adhesion. Since water is the universal solvent for life, and the main solvent in the environment and industry, water was chosen as the model liquid. In the calculations of interfacial tensions (presented in equations 2-4) and Gibbs free energy change (equation 1), the surface tensions of Si_3N_4 and water were taken as 56 mJ/m^2 and 73 mJ/m^2 [26], respectively. The surface tensions of the bacterial cells were determined using the spectrophotometric method as described above. In addition to the calculations of Gibbs free energy changes for the adhesion of WT cells and FliA mutants to Si_3N_4 surfaces in water (ΔG_{adh}), the Gibbs free energy changes for auto-adhesion (WT-to-WT and mutant-to-mutant) and co-adhesion (WT-to-mutant or mutant-to-WT) in water were also calculated. For those calculations, the surface tension of the solid presented in equations 1-4 was replaced by the surface tension of the WT strain or FliA mutant strain to determine $\Delta G_{auto\text{-}adh}$ (mJ/m^2) and $\Delta G_{co\text{-}adh}$ (mJ/m^2).

AFM Measurements

Samples were prepared by attaching WT cells and FliA mutants to poly-L-lysine (PLL)-coated mica disks following the procedure described previously [31]. Then the scanning and force measurements were performed on the samples using Hitachi AFM5100N atomic force microscope (Hitachi High-Tech Corp.), and Si_3N_4 AFM probes (DNP-S probes, 0.24 N/m, Bruker AXS Inc.). The images of bacterial cells were captured at dynamic fluid mode (DFM or tapping mode) using a scan rate of 0.50 Hz and line pixels of 256 lines (Figure 1).

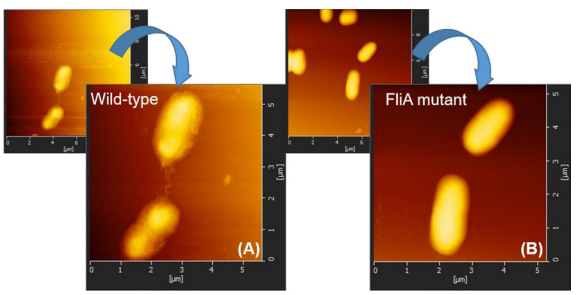

Figure 1. AFM images of (A) *E. coli* MG1655 wild-type (WT) cells, and (B) *E. coli* MG1655 FliA mutants in water captured at dynamic fluid mode (DFM mode).

When measuring force-distance curves, the probe of the AFM approaches to a spot on the sample surface, contacts with the surface, and then moves away from the surface perpendicularly. As this happens, the AFM detects and measures the interaction forces between the probe and the spot on the sample surface as a function of the distance the probe moves. In this way, force-distance curves were measured at 10 different spots on a bacterial cell and 6 bacterial cells each from WT and mutant strains were selected for the measurements. For adhesion measurements, data recorded as the probe moved away from the sample (retraction curves) were used. A total of 60 retraction force-distance curves (6 bacterial cells × 10 different points on each cell) were measured and analyzed to obtain irreversible bacterial adhesion energy at the nano-scale for each bacterial group studied.

Analysis of AFM Retraction Force-Distance Curves

The cell surface-associated macromolecules often attach to the AFM probe at the spot where the AFM probe contacts the surface of the bacterium. As the probe moves away from the surface, the molecules detach from the probe, and single or multiple adhesion peaks or so called pull-off force peaks are observed (Figure 2). Unlike AFM images, significant processing and analysis is often required to extract meaningful information from the force-distance curves. In this study, 60 retraction-force-distance curves were analyzed for each investigated to quantify the irreversible bacterial adhesion energy to the Si_3N_4 surface in water by approximating the integral below using the trapezium method:

$$E_{adh}(AFM) = -\int_{x_1}^{x_2} F dx \approx -\frac{x_2 - x_1}{n}\left(\frac{F(x_1)+F(x_2)}{2} + \sum_{k=1}^{n-1} F(x_1 + k\frac{x_2 - x_1}{n})\right) \quad (5)$$

In equation 5, E_{adh} (AFM) represents the irreversible bacterial adhesion energy computed from the recorded AFM data, F is the pull-off force (when multiplied by the negative value, adhesion force is obtained), x is the distance and n is the number of data points in the integral interval. After the analysis of retraction curves, the mean, standard error (SE) of the mean and the median values of the adhesion energies were quantified.

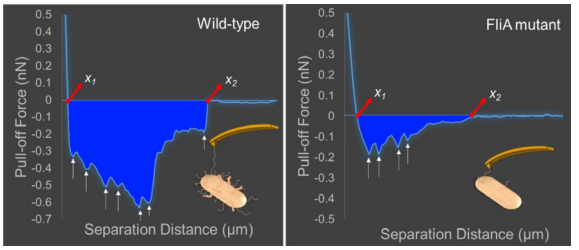

Figure 2. Examples of retraction force-distance curves obtained after force measurement at a single spot on each of the bacterial cells. Bacterial irreversible adhesion energy was obtained by calculating the blue area using equation 5. The arrows indicate the adhesion peaks.

Determination of Bacterial Surface Heterogeneity

Since adhesive cell surface molecules are heterogeneous [32], different types of adhesion peaks can be seen in the retraction curves (Figure 2) depending on what binds the probe and the sample. Hence, the commonly observed heterogeneity in adhesion forces and/or energies can be used to describe heterogeneity in bacterial surface macromolecules [14, 26, 28, 31, 33]. In this study, the frequency histograms of adhesion energies were generated to determine the bacterial surface heterogeneity. The ranges of the frequency distributions were obtained and used as indicators of surface heterogeneity. Furthermore, bacterial surface heterogeneity was determined by a heterogeneity index (HI). As presented in equation 6, HI was defined as the ratio of the standard error (SE) of the mean value obtained for the adhesion energy data to the highest SE of the mean obtained for the data set [33].

$$HI = \frac{\text{SE of the mean}}{\text{Max. SE of the mean}} \quad (6)$$

Analysis of Bacterial Surface Roughness

The surfaces of WT cells and FliA mutants can be compared in terms of average surface roughness and root-mean-square (RMS) surface roughness, the two most common roughness parameters that affect the available bacterial surface area required for the adhesion [34]. The average surface roughness (R_a) is the arithmetical mean of the absolute values of the height deviations from the mean, whereas RMS surface roughness (R_q) is the square root of the sum of the squares of the values of the height deviations from the mean. The R_a and R_q values were determined for each of the bacterial strains studied using the AFM software.

Statistical Analysis

Mann-Whitney Rank Sum test and t-test were applied to determine whether there were statistically significant differences in the adhesion energies and surface roughness parameters, respectively.

RESULTS AND DISCUSSION

Since bacterial cells have similar dimensions to colloidal particles, can disperse throughout the medium and scatter light, the stability of a bacterial suspension can be predicted using the Derjaguin-Landau-Verwey-Overbeek (DLVO) colloidal stability theory [14, 15]. DLVO theory states that the physiochemical interactions between two surfaces are dominated by attractive Lifshitz-van der Waals (LW) and repulsive electrostatic interactions and that the balance of the two interactions determines colloidal stability. Based on this theory, it can be predicted that when the least attractive LW interaction is observed, bacterial cells will be maximally dispersed in the liquid medium, leading to a minimal amount of sedimentation. When the bacterial cells are maximally dispersed in the liquid, which can be identified from the highest OD value of the cell suspension (Figure 3A and 3B), their surface tension should be close to the surface tension of the liquid they are in [20-22]. The results showed that the peak OD values corresponding to the surface tensions of the bacterial cells were 57 mJ/m² and 60 mJ/m² for the WT and FliA mutant strains, respectively (Figure 3A and 3B). The bacterial surface tensions determined in this study were in good agreement with literature values obtained

for various strains of *E. coli* using conventional contact angle measurements with water and the equation of state approach, or using contact angle measurements with water, formamide and α-bromonapthalene and the LW-AB approach [35].

To quantify the Gibbs free energy change (equation 1) for bacterial adhesion to Si_3N_4 (solid surface) in water (liquid), the interfacial tensions of the interacting surfaces (presented in equations 2-4) were calculated using the surface tensions of the bacterial cells obtained by the spectrophotometric measurements. As described in the theory of surface thermodynamics, spontaneous bonding occurs with a decrease in the free energy of the process, so adhesion is favored if the free energy per area is negative [23-26]. Therefore, when $\Delta G_{adhesion}$ (mJ/m²) is negative, bacterial adhesion is thermodynamically favorable, and will progress spontaneously [23-26]. The values of Gibbs free energy change obtained for the adhesion of WT and FliA mutant strains to Si_3N_4 in water (ΔG_{adh}) were negative (Figure 3C), indicating that the reversible adhesion of both of the strains to Si_3N_4 in water was a thermodynamically favorable process. This finding suggests that cells lacking flagella and other FliA-dependent surface macromolecules will be able to overcome the repulsive forces near an inert surface such as Si_3N_4 in water and adhere to the surface reversibly. However, in comparison, the negative Gibbs free energy change quantified for the reversible adhesion of the WT strain (-10.2 mJ/m²) was higher than that quantified for the mutant strain (-8.36 mJ/m²), suggesting that the reversible adhesion of the WT strain to Si_3N_4 in water is more favorable. During biofilm formation, planktonic bacterial cells will not only approach and attach to the bare substrate but also to the cells that have already managed to attach to the surface. Therefore it is also significant to investigate the reversible bacterial auto-adhesion (adhesion between microbial pairs from the same strain) as well as co-adhesion (adhesion between microbial pairs from different strains) [24, 25]. To quantify the Gibbs

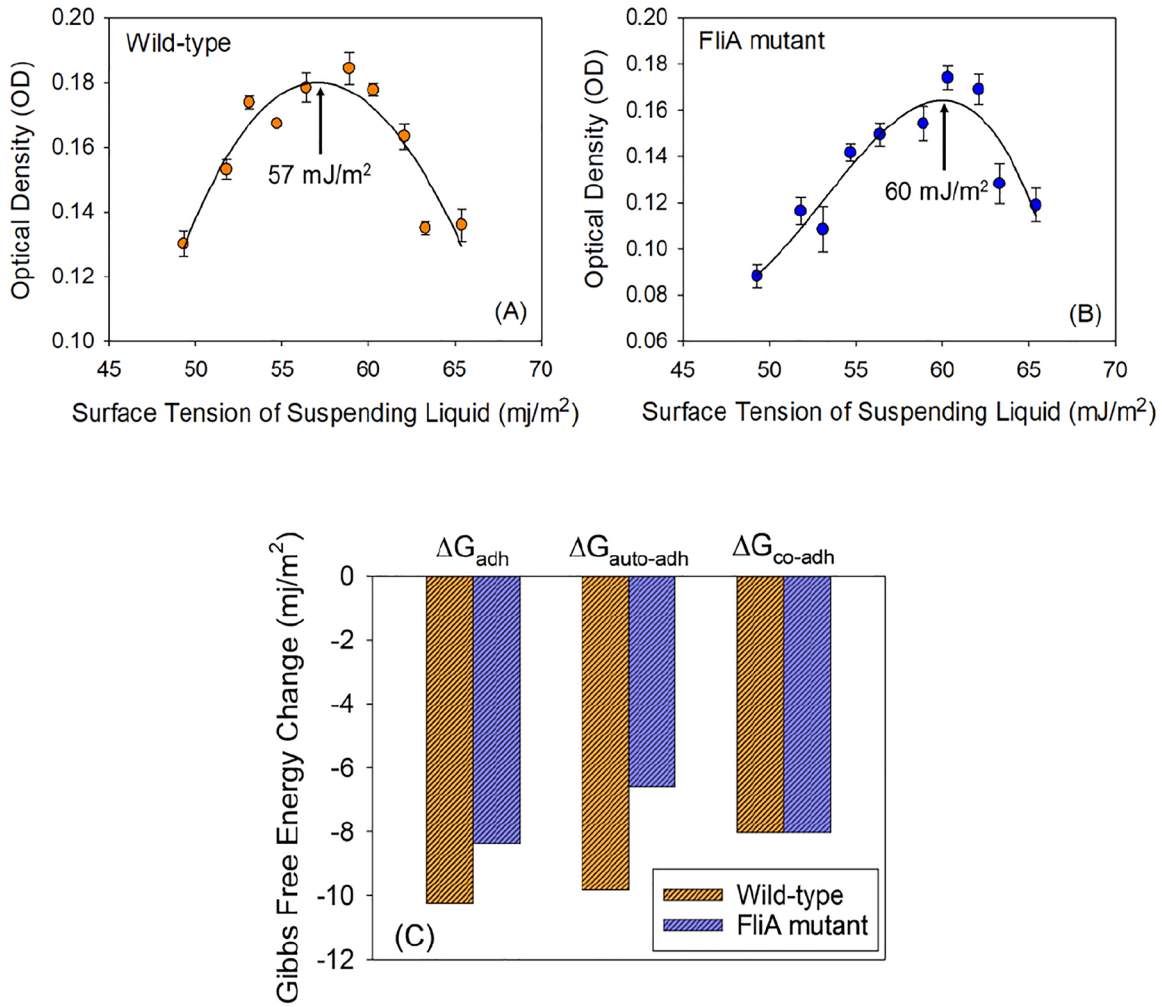

Figure 3. Plots of the optical densities (OD 570 nm) measured for the suspensions of (A) *E. coli* wild-type (WT) strain and (B) FliA mutant strain as functions of surface tensions of the suspending ethanol-water mixtures. Straight lines indicate the polynomial fitting. (C) Gibbs free energy changes for adhesion between WT strain-Si_3N_4 and mutant strain-Si_3N_4 (ΔG_{adh}), auto-adhesion between WT-WT strains and mutant-mutant strains ($\Delta G_{auto\text{-}adh}$), and co-adhesion between WT-mutant strains or mutant-WT strains ($\Delta G_{co\text{-}adh}$).

free energy changes for bacterial auto-adhesion ($\Delta G_{auto\text{-}adh}$) and co-adhesion ($\Delta G_{co\text{-}adh}$) in water, the surface tension of the solid presented in equations 1-4 was replaced by the surface tension of the WT strain or the FliA mutant strain. As presented in Figure 3C, the auto-adhesion between the WT cells ($\Delta G_{auto\text{-}adh}$ = -9.82 mJ/m²) was more thermodynamically favorable than the co-adhesion between the WT and mutant cells ($\Delta G_{co\text{-}adh}$ = -8.04 mJ/m²) and auto-adhesion between the mutant cells ($\Delta G_{auto\text{-}adh}$ = -6.58 mJ/m²), respectively, showing the positive impact of FliA-dependent surface macromolecules on the reversible bacterial auto-adhesion and co-adhesion during the first step of biofilm formation of *E. coli*.

To investigate the role of FliA-dependent surface macromolecules in the initial irreversible adhesion of *E. coli* as well as the heterogeneity of the surface macromolecules, atomic force microscopy (AFM) measurements were performed on the WT and FliA mutant cells. In the irreversible bacterial attachment to the surface, bacterial cells bind to the surface via their adhesive cell surface-associated macromolecules [10-14]. Thus, it can be said that the more the bacterial surface is covered by different types of adhesive surface macromolecules, which can be judged by the heterogeneity of the cell surface, the greater the strength of irreversible bacterial adhesion to the surface. In this study, bacterial surface heterogeneity was defined by the ranges of distributions in the frequency histograms of measured AFM adhesion energies and the values of heterogeneity indexes [33]. The frequency distribution of the adhesion energies measured between Si_3N_4 probes and WT cells in water (Figure 4A) was wider than the distribution obtained for the FliA mutant cells (Figure 4B).

In comparison, the range quantified for the frequency distribution of adhesion energies of the WT cells was 4.8-fold wider than the range of that obtained for the FliA mutant cells (Table 1). Similarly, the heterogeneity index (HI) quantified for the WT cells was approximately 5.5-fold higher than the HI quantified for the mutants (Table 1). These findings support the fundamental role for FliA in the synthesis of *E. coli* surface macromolecules, all of which contribute to *E. coli* surface heterogeneity. Furthermore, the measured adhesion energies for the WT and mutant cells were different from each other (Figure 4C, $p < 0.001$). In comparison, the mean and the median values of the measured adhesion energies for the WT cells were approximately 3.2-fold and 2.0-fold greater than the mean and the median adhesion energies for the mutant cells, respectively (Table 1). These results show that the irreversible adhesion strength of WT cells to Si_3N_4 in water is at least 2.0-fold greater than that of the FliA mutants due to the higher amount and/or diversity of their adhesive surface molecules, leading to higher surface heterogeneity.

The role of FliA-dependent surface macromolecules in the roughness of the cell surface was also investigated using the captured images by the AFM. Statistical comparison indicated that surface roughness parameters (R_a and R_q, respectively) obtained for the WT and FliA mutant cells were different from each other (Figure 4D, $p = 0.019$ and p = 0.014, respectively). As presented in Table 1 and Figure 4D, R_a and R_q values obtained for the WT cells were on average 2-fold higher than those obtained for the FliA mutant cells. The higher cell surface roughness observed for the WT cells was in line with their higher surface heterogeneity which indicated a more heterogeneous population of surface macromolecules for the WT cells compared to the mutant cells. Previous studies have shown that it is easier for bacterial cells with a rougher surface to adhere firmly to a substratum surface [36, 37] and that rougher bacterial surfaces promote attractive van der Waals forces mediating the adhesion between the bacteria and surfaces [36]. Therefore, it can be concluded that the higher irreversible adhesion energy obtained for the WT cells was probably due to their higher surface heterogeneity resulting in higher surface roughness for the WT cells.

Table 1. Results obtained after direct measurements by AFM and analysis of the measured data showing the mean, standard error (SE) of the mean, median, range and the heterogeneity index (HI) of the energies presented in the frequency distributions, and the roughness parameters for the bacterial surfaces.

	AFM Adhesion Energy (aJ)					**Surface Roughness (nm)**	
	Mean	SE of Mean	Median	Range	HI	R_a	R_q
Wild-type	51.4	6.5	31.0	156.7	1.00	31.3 ± 5.2	40.1 ± 6.6
FliA mutant	16.0	1.2	15.1	32.5	0.18	15.5 ± 6.4	18.9 ± 7.4

CONCLUSION

Understanding the effects of specific bacterial surface macromolecules and the specific regulatory components involved in their synthesis on biofilm development may lead to the design of novel molecules, molecule inhibitors, surface coatings and surface modifications that can reduce bacterial adhesion and biofilm development. In this context, this study provides important insights into the effect of FliA-dependent surface macromolecules on the surface properties of *E. coli* and their impact on the initial biofilm development steps consisting of reversible and irreversible adhesion of *E. coli* to the surface of the model

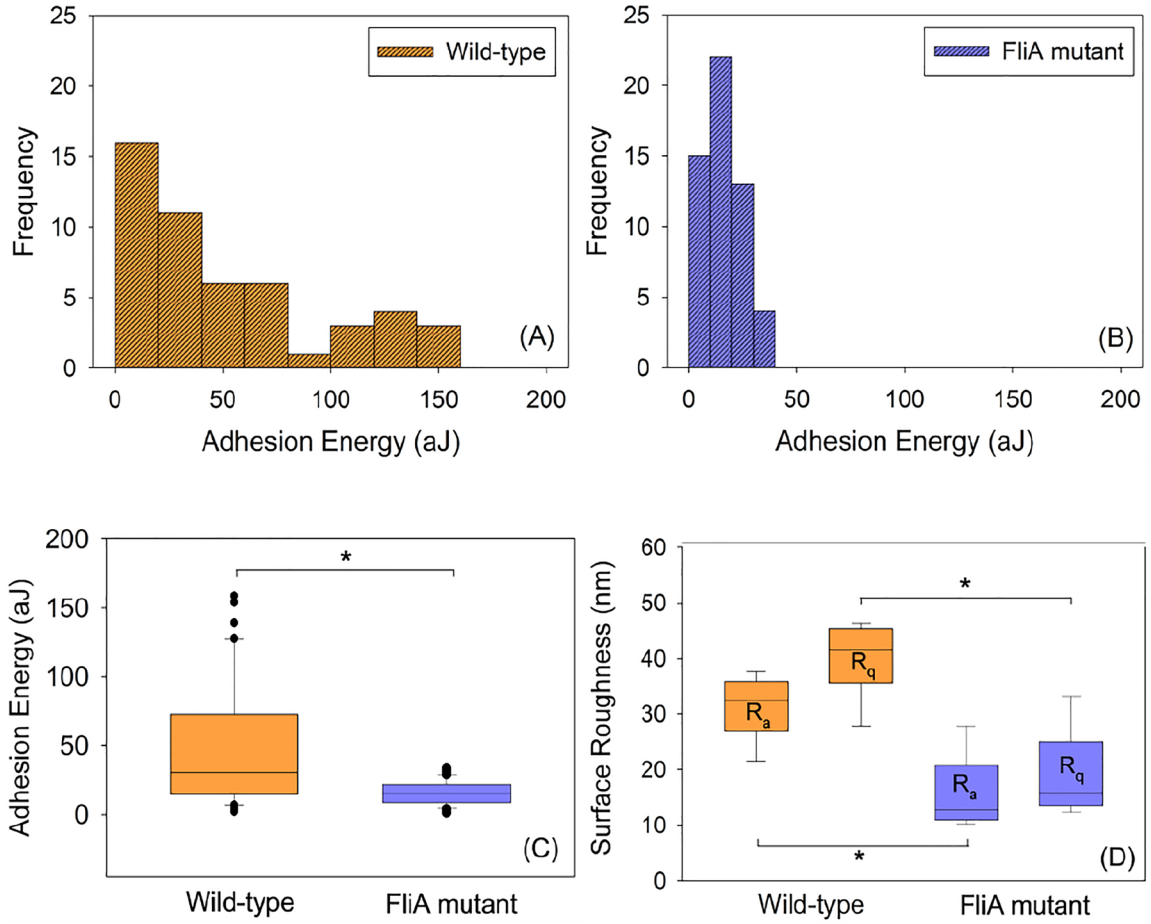

Figure 4. Frequency distributions of adhesion energies (aJ) measured between Si_3N_4 AFM probes and (A) *E. coli* wild-type (WT) cells and (B) *E. coli* FliA mutants in water. (C) Box plot of measured bacterial adhesion energies. Black points in the box plot indicate 5th/95th percentile outliers (*p < 0.001, Mann-Whitney Rank Sum Test). (D) Box plot of average (R_a) and RMS (R_q) surface roughness parameters of the bacterial cells (*p < 0.05, t-test).

solid, inert Si_3N_4, in water. The results obtained in this study suggest a combined method, such as modifying the surface of interest with a bacterial repellent layer capable of reducing attractive van der Waals interactions and targeting FliA-dependent surface macromolecules to reduce reversible adhesion, auto-adhesion, and co-adhesion as well as irreversible adhesion of *E. coli*. The methods used and the results obtained in this study may also guide the studies investigating the adhesion of *E. coli* WT and mutant cells to other inert surfaces as well as the studies investigating the role of FliA in the surface properties and initial biofilm development of other microorganisms.

ACKNOWLEDGMENTS

The author would like to thank to Dr. Colin Grant, former HITACHI SPM Product Manager (Europe), for his technical support on the AFM measurements.

CONFLICT OF INTEREST

The study was conducted by only one author. The author declares that there are no known conflicts of interest.

REFERENCES

1. Bridier A, Briandet R, Thomas V, Dubois-Brissonnet F. Resistance of bacterial biofilms to disinfectants: a review. Biofouling 27 (2011) 1017-1032.
2. Davies D. Understanding biofilm resistance to antibacterial agents. Nature Reviews Drug Discovery 2 (2003) 114–122.
3. Donlan RM, Costerton JW. Biofilms: survival mechanisms of clinically relevant microorganisms. Clinical Microbiology Reviews 15 (2002) 167-193.
4. Sharma G, Sharma S, Sharma P, Chandola D, Dang S, Gupta S, Gabrani R. *Escherichia coli* biofilm: development and therapeutic strategies. Journal of Applied Microbiology 121 (2016) 309-319.

5. Devanga Ragupathi NK, Veeraraghavan B, Karunakaran E, Monk PN. Editorial: Biofilm-mediated nosocomial infections and its association with antimicrobial resistance: detection, prevention, and management. Frontiers in Medicine (Lausanne) 9 (2022) 987011.
6. Aslam B, Wang W, Arshad MI, Khurshid M, Muzammil S, Rasool MH, Nisar MA, Alvi RF, Aslam MA, Qamar MU, Salamat MKF, Baloch Z. Antibiotic resistance: a rundown of a global crisis. Infection and Drug Resistance 11 (2018) 1645-1658.
7. Wingender J, Flemming HC. Biofilms in drinking water and their role as reservoir for pathogens. International Journal of Hygiene and Environmental Health 214 (2011) 417-423.
8. Galié S, García-Gutiérrez C, Miguélez EM, Villar CJ, Lombó F. Biofilms in the food industry: health aspects and control methods. Frontiers in Microbiology 9 (2018) 898.
9. Reisner A, Maierl M, Jörger M, Krause R, Berger D, Haid A, Tesic D, Zechner EL. Type 1 fimbriae contribute to catheter-associated urinary tract infections caused by *Escherichia coli*. Journal of Bacteriology 196 (2014) 931-939.
10. Ballén V, Cepas V, Ratia C, Gabasa Y, Soto SM. Clinical *Escherichia coli*: from biofilm formation to new antibiofilm strategies. Microorganisms 10 (2022) 1103.
11. Beloin C, Roux A, Ghigo JM. *Escherichia coli* biofilms. Current Topics in Microbiology and Immunology 322 (2008) 249-289.
12. Buck LD, Paladino MM, Nagashima K, Brezel ER, Holtzman JS, Urso SJ, Ryno LM. Temperature-dependent influence of FliA overexpression on PHL628 *E. coli* biofilm growth and composition. Frontiers in Cellular and Infection Microbiology 11 (2021) 775270.
13. Friedlander RS, Vogel N, Aizenberg J. Role of flagella in adhesion of *Escherichia coli* to abiotic surfaces. Langmuir 31 (2015) 6137-44.
14. Gordesli FP, Abu-Lail NI. Combined Poisson and soft-particle DLVO analysis of the specific and nonspecific adhesion forces measured between L. monocytogenes grown at various temperatures and silicon nitride. Environmental Science & Technology 46 (2012) 10089-98.
15. Israelachvili JN. Intermolecular and Surface Forces, third ed. Academic Press, New York, 2011.
16. Claret L, Miquel S, Vieille N, Ryjenkov DA, Gomelsky M, Darfeuille-Michaud A. The flagellar sigma factor FliA regulates adhesion and invasion of Crohn disease-associated *Escherichia coli* via a cyclic dimeric GMP-dependent pathway. The Journal of Biological Chemistry 282 (2007) 33275-33283.
17. Fitzgerald DM, Bonocora RP, Wade JT. Comprehensive mapping of the *Escherichia coli* flagellar regulatory network. PLoS Genetics 10 (2014) e1004649.
18. Pesavento C, Becker G, Sommerfeldt N, Possling A, Tschowri N, Mehlis A, Hengge R. Inverse regulatory coordination of motility and curli-mediated adhesion in *Escherichia coli*. Genes & Development 22 (2008) 2434-46.
19. Wood TK, Barrios AFG, Herzberg M, Lee J. Motility influences biofilm architecture in *Escherichia coli*. Applied Microbiology and Biotechnology 72 (2006) 361-367.
20. Zhang X, Jiang Z, Li M, Zhang X, Wang G, Chou A, Chen L, Yan H, Zuo YY. Rapid spectrophotometric method for determining surface free energy of microalgal cells. Analytical Chemistry 86 (2014) 8751-8756.
21. Zhang X, Zhang Q, Yan T, Jiang Z, Zhang X, Zuo YY. Surface free energy activated high-throughput cell sorting. Analytical Chemistry 86 (2014) 9350-9355.
22. Zhang X, Zhang Q, Yan T, Jiang Z, Zhang X, Zuo YY. Quantitatively predicting bacterial adhesion using surface free energy determined with a spectrophotometric method. Environmental Science & Technology 49 (2015) 6164-6171.
23. Absolom DR, Lamberti FV, Policova Z, Zingg W, van Oss CJ, Neumann AW. Surface thermodynamics of bacterial adhesion. Applied Environmental Microbiology 46 (1983) 90-97.
24. Bos R, van der Mei HC, Busscher HJ. Physico-chemistry of initial microbial adhesive interactions-its mechanisms and methods for study. FEMS Microbiology Reviews 23 (1999) 179–230.
25. Carniello V, Peterson BW, van der Mei HC, Busscher HJ. Physico-chemistry from initial bacterial adhesion to surface-programmed biofilm growth. Advances in Colloid and Interface Science 261 (2018) 1-14.
26. Park BJ, Abu-Lail NI. The role of the pH conditions of growth on the bioadhesion of individual and lawns of pathogenic Listeria monocytogenes cells. Journal of Colloid and Interface Science 358 (2011) 611-620.
27. Kwok DY, Neumann AW. Contact angle measurement and contact angle interpretation. Advances in Colloid and Interface Science 81 (1999) 167–249.
28. Abu-Lail NI, Camesano TA. Role of lipopolysaccharides in the adhesion, retention, and transport of *Escherichia coli* JM109. Environmental Science & Technology 37 (2003) 2173-2183.
29. Borer B, Tecon R, Or D. Spatial organization of bacterial populations in response to oxygen and carbon counter-gradients in pore networks. Nature Communications 9 (2018) 769.
30. Du X, Lee SS, Blugan G, Ferguson SJ. Silicon nitride as a biomedical material: an overview. International Journal of Molecular Sciences 23 (2022) 6551.
31. Ordek A, Gordesli-Duatepe FP. Impact of sodium nitroprusside concentration added to batch cultures of *Escherichia coli* biofilms on the c-di-GMP levels, morphologies and adhesion of biofilm-dispersed cells. Biofouling 38 (2022) 796–813.
32. Moradali MF, Rehm BHA. Bacterial biopolymers: from pathogenesis to advanced materials. Nature Reviews Microbiology 18 (2020) 195–210.
33. Park BJ, Abu-Lail NI. Atomic force microscopy investigations of heterogeneities in the adhesion energies measured between pathogenic and non-pathogenic Listeria species and silicon nitride as they correlate to virulence and adherence. Biofouling 27 (2011) 543-559.
34. Laskowski D, Strzelecki J, Pawlak K, Dahm H, Balter A. Short communication effect of ampicillin on adhesive properties of bacteria examined by atomic force microscopy. Micron 112 (2018) 84–90.
35. Sharma PK, Rao KH. Analysis of different approaches for evaluation of surface energy of microbial cells by contact angle goniometry. Advances in Colloid and Interface Science 98 (2002) 341-463.
36. Shao W, Liu H, Liu X, Wang S, Zhang R. Anti-bacterial performances and biocompatibility of bacterial cellulose/graphene oxide composites. RSC Advances 5 (2015) 4795-4803.
37. Uzoechi SC, Abu-Lail NI. The effects of β-lactam antibiotics on surface modifications of multidrug-resistant *Escherichia coli*: a multiscale approach. Microscopy and Microanalysis 25 (2019) 135-150.
38. Vu B, Chen M, Crawford RJ, Ivanova EP. Bacterial extracellular polysaccharides involved in biofilm formation. Molecules 14 (2009) 2535–2554.